Pool Boiling Enhanced by Electric Field Distribution in Microsized Space

Ichiro Kano [1,*]

* Corresponding author: Tel.: +81 (238) 26 3226; Fax: +81 (238) 26 3226; Email: kano@yz.yamagata-u.ac.jp
[1] Graduate School of Science and Engineering, Yamagata University, JPN

Abstract In this study, the enhancement of boiling heat transfer by electrostatic pressure was experimentally and analytically investigated. A fluorinated dielectric liquid was selected as the working fluid. Pool boiling heat transfer in the saturated liquid was measured at atmospheric pressure. In order to make clear the enhancement mechanisms, three microsized slit electrodes were designed with different slit widths, electrode widths, and total slit lengths over the boiling surface. Slits of several hundred micrometers were formed in the electrode, so as to remove vapor bubbles from the boiling surface by electrostatic pressure. The boiling surface was electrically grounded, and the electrode was placed above the boiling surface at heights of 200 μm to 400 μm. The maximum heat flux was 76 W/cm^2 by the application of an electric field of −7 kV/mm, which was 3.5 times over pool boiling without the electrode. The previous analytical equation of pool boiling exhibited the essential feature of the effect of the electric field on the boiling heat transfer, and showed good agreement with the experimental results.

Keywords: Boiling, Electric Field, Heat Transfer Enhancement, Microsized Space

1. Introduction

Thermal management of high-power electronic systems such as high-output broadcasting amplifiers and laser diodes requires heat dissipation of more than 100 W/cm^2. Dielectric liquids are an attractive means of cooling electrical components because they are chemically inert and have very low electrical conductivities. However, the thermal management capabilities of dielectric liquids, such as their specific and latent heat, are lower than those of water. Therefore, a cooling system using a dielectric liquid must be larger than a water management system used for cooling, because the flow rate must be increased.

Boiling heat transfer is another means of cooling. It may be viable for cooling electric components, but only if an innovative design is produced to manage the currently uncontrolled increase in wall temperature at the critical heat flux (CHF). It may be possible to control this temperature increase by using electrohydrodynamic (EHD) effects. EHD effects produce pressure and net flow when a dielectric liquid is exposed to high voltage. Pumping designs that produce EHD effects have the advantages of no moving parts, simple designs, and low weights. For these reasons, a number of theoretical and experimental investigations of this pumping design have been performed since the early 1960s (e.g., Stuetzer, 1959; Pickard, 1963; Pickard, W. F., 1963). Following these experimental and theoretical works, others reviewed the EHD mechanisms in detail (e.g., Saville, 1997). Several researchers have recognized EHD as an efficient, active method of increasing heat exchange (Jones, 1978; Marco and Grassi, 1993; Allen and Karayiannis, 1994; Laohalertdecha et al., 2007). Hristov et al. (2009) successfully increased the CHF for the saturated boiling of R123 on a polished copper wall from 20 W/cm^2 without the electric field to 64.6 W/cm^2 by the application of a high dc voltage of 25 kV.

When the dielectric liquid (permittivity ε_l) is confined in a pair of parallel electrodes and a uniform electric field is applied to the liquid, the liquid rises between the electrodes because

Nomenclature

A	Boiling surface area [m^2]	λ	Wavelength [m]
E	Electric field [V/m]	λ_d	Wavelength between vapor columns [m]
H	Electrode height [m]	ρ	Mass density [kg/m^3]
L	Latent heat [kJ/kg]	σ	Surface tension [N/m]
l_n	Slit length [m]		
Ls	Total slit length [m]	Subscriptions	
P	Pressure [Pa]	ESP	Electrostatic pressure
W_e	Electrode width [m]	g	Gas
W_S	Slit width [m]	l	Liquid
ε	Dielectric permittivity [F/m]	v	Vapor

of the Maxwell stress tensor acting on the liquid–gas interface (Panofsky, 1962). The electrostatic pressure difference ΔP_{ESP} is given by

$$\Delta P_{ESP} = \frac{1}{2}(\varepsilon_l - \varepsilon_g)E^2. \quad (1)$$

An application of the electrostatic pressure to the microfabricated cooling device was reported by Darabi et al. (2001). The maximum cooling capacity of 65 W/cm^2 was achieved using R-134a. Further work resulted in the development of a thin-film evaporator driven by the electrostatic force (Darabi and Ekula, 2003; Moghaddam and Ohadi, 2005). The use of microsplayed geometry using microfabrication technology significantly enhanced pumping power, and achieved a maximum heat flux of 35 W/cm^2.

Based on these studies and the many advantages of electric field application, it was possible to study pool boiling enhanced by electric field application using micropatterned interdigital electrodes (Kano and Takahashi, 2013). In a subsequent study (Kano et al., 2013), it was found that electrostatic pressure effectively increased CHF and that CHF continued to increase to 47 W/cm^2 using a microsized slit electrode. The author then proposed a boiling heat transfer enhancement model, as shown in Fig. 1 (Kano, 2014). A microsized electrode, with slits of 700 μm in width, was installed over the boiling surface with the application of high dc voltages. At

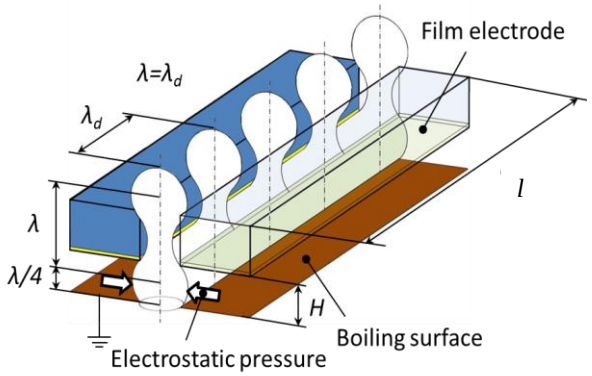

Fig. 1. Vapor removal configuration for boiling around slit electrodes

high superheat, an interface between the liquid and vapor, resulting from the combination of the nucleate bubbles, was created in the gaps between the boiling surface and the electrode. Electrostatic pressure was generated at the interface and continually supplied the liquid to the boiling surface. Oscillation of the interface at the bottom rim of the boiling bubble periodically crate a thin liquid film, which periodically evaporated, strongly increasing the heat flux. From this experiment, a mathematical expression to predict maximum heat flux was derived based on the addition of electrostatic pressure to the hydrodynamic theory as follows:

$$q_{\max,EHD} = \frac{\pi\lambda}{48} L\rho_v \frac{Ls}{A} \times \left[\frac{\rho_l + \rho_v}{\rho_l \rho_v} \left\{ \frac{2\pi\sigma}{\lambda} + E^2 (\varepsilon_l - \varepsilon_v) \tanh\left(\frac{2\pi X_0}{\lambda} \right) \right\} \right]^{\frac{1}{2}}, \quad (2)$$

where λ is the wavelength, which depends on the electrode height H;

$$\lambda = 2H, \quad (3)$$

X_0 is the position at the liquid–gas interface under the electrode;

$$X_0 = We/2, \quad (4)$$

And Ls is the total slit length, which is determined by

$$Ls = \sum_{n=1}^{N} l_n, \quad (5)$$

where l_n is the length of each slit over the boiling surface and N is the number of slits (Kano, 2014). Fig. 2 depicts the electrode geometry.

According to Eq. (2), the critical heat flux should increase with the electric field E, wavelength λ (= 2H), and total slit length Ls.

In a Previous study, the author measured the boiling heat flux in a saturated dielectric liquid (Asahi Glass Co. Ltd., AE-3000) and successfully increased the CHF from 22 W/cm^2 of pool boiling without the electrode to 86 W/cm^2 at H = 600 μm with the application of −3000V (Kano, 2014). However, the experimental values deviated slightly from the calculated values of Eq. (2) because of a slight difference between the experimental and model electrode configurations.

This paper deals with the enhancement of boiling heat transfer by electrostatic force with a very simple electrode configuration, which is intended to help clarify the enhancement mechanisms. The effects of the electric field E, wavelength λ (= 2H) and total slit length Ls on the CHF were studied, and the experimental results were compared with the theoretical results of Eq. (2).

2. Experimental Facility

The experimental facilities have been described in a previous study (Kano, 2014). In this paper, a summary of the main experimental facilities are described, and electrode devices that have the same configuration as that of the analytical model are presented in detail.

To create a uniform high electric field and produce electrostatic pressure over the boiling surface, microsized electrodes were used (as shown in Fig. 2) in three electrode configurations. The detailed size of configurations A1, A2, and A3 are shown in Table 1. The slit width, *Ws*, was changed from 400 to 500μm that were larger than the bubble size at departure (168 μm) calculated by the

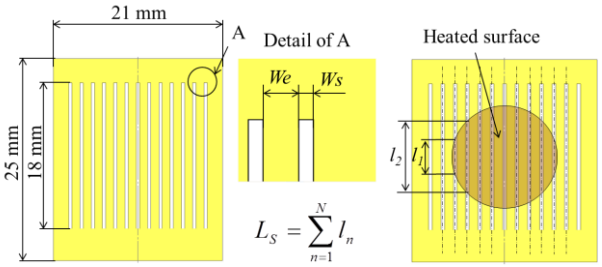

Fig. 2. Present electrode geometry (thickness is 1 mm)

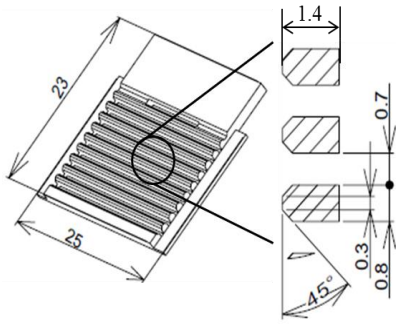

Fig. 3. Previous electrode geometry (dimensions in mm)
(Kano, 2014 and Kano et al., 2013)

Table 1
List of electrode structures, divided by electrode width, slit width, and total slit length.

Electrode	*We* (μm)	*Ws* (μm)	*Ls* (mm)
A1	1000	400	128
A2		500	114
A3	1500	500	87
Kano, 2014 Kano et al., 2013	800	700	114

Table 2
Properties of the working liquid at 1 atm.

Property	AE-3000 CF3CH2OCF2CHF2
Boiling point (°C)	55.5
Dielectric strength (kV/mm)	16
Electric conductivity (S/m) at 23°C	7.7×10^{-10}
Latent heat (kJ/kg) at 55.5°C	147
Liquid density (kg/m^3) at 55.5°C	1,393
Liquid viscosity (mPas) at 25°C	0.646
Liquid permittivity (-) at 25°C	7.2
Surface tension (mN/m) at 55.5°C	12.20
Vapor density (kg/m^3) at 55.5°C	7.82

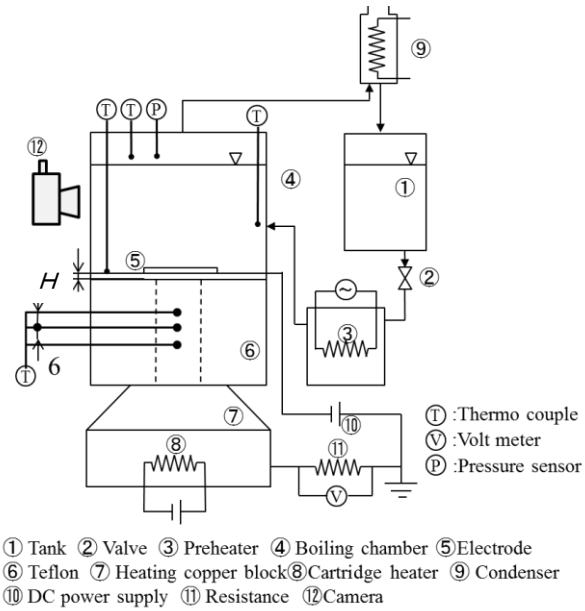

Fig. 4. Schematic of the experimental facility (dimensions in mm)

Frits and Wark equation (Tong and Tang, 1997). The electrode width *We* was changed from 1,000 to 1,500 μm. The total slit length *Ls* was changed from 87 mm to 128 mm. The electrode was 21 mm × 25 mm × 1 mm, allowing Cr/Au (800 Å/3000 Å) deposit over an entire substrate made of synthetic silica. The silica deposited with Cr/Au was slit by a dicing saw (Disco Co., DAD322), which was precisely controlled by programing to avoid chipping the surface. In order to determine the effect of the electrode configuration on pool boiling, the author compared the results with previous experimental results (Kano, 2014; Kano et al., 2013). A stainless steel electrode was used, as shown in Fig. 3, and its edge was planed to 250 μm. The detailed electrode size is listed in Table 1; *We*, *Ws*, and *Ls* were 800μm, 700 μm, and 114 mm, respectively.

AE-3000 (Asahi Glass Co., Ltd.) was used as the working fluid in the experiments. This liquid has a permittivity of 7.2 and a relatively low viscosity. The other properties of this fluid are listed in Table 2.

The experimental facilities are illustrated in Fig. 4. The system was operated at atmospheric pressure by opening the top of the condenser. The condenser was cooled by circulating water chilled by a refrigeration system. The rectangular boiling chamber (internal dimensions 50 mm × 50 mm × 50 mm) was made of 10-mm-thick transparent polycarbonate. The boiling process occurred on the 15-mm-diameter top surface of an oxygen-free copper block, which was 38 mm long. The side of the block was insulated with Teflon. Five 100 W electric cartridge heaters were embedded in the bottom of the copper block, which was electrically connected in parallel (total resistance was 20 Ω). The temperature gradient in the copper block was measured with an uncertainty of 0.04 K by three T-type thermocouples insulated by 1/16 in. diameter ceramic (Omega Eng. Inc., TRM-164116-6). The thermocouples were inserted 7.5 mm deep and at 13.0 mm, 19.0 mm, and 25.0 mm from the boiling surface. The temperature field inside the copper block was one-dimensional, and the heat flux was calculated from the temperature gradient with a maximum uncertainty of ± 0.27 W/cm^2.

The average copper surface roughness Ra was reduced to 0.03－0.05 μm by polishing with a 3M lapping film sheet (#2000).

The working fluid was boiled at a moderate heat flux for 120 min to remove any remaining trapped air. Boiling curves were obtained by increasing the heat flux provided by the cartridge heater with intervals of 0.05A current. Then, the heat flux was increased with the increase in electric power of the heat cartridge. Data, including current and voltage measurements, thermocouple outputs, and vessel pressure were logged for 3 min 10 s at 10 s intervals after reaching steady conditions.

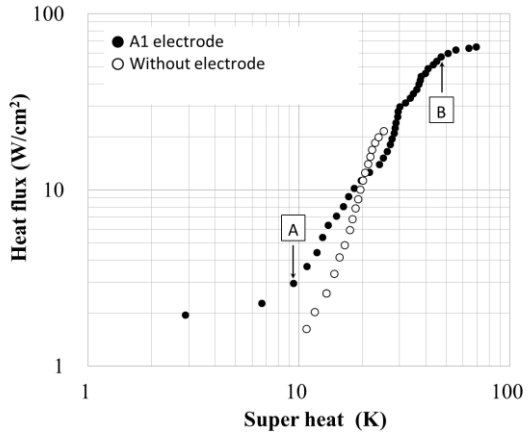

Fig. 5. Heat flux as a function of wall superheat at H = 400 μm and E= −5 kV/mm

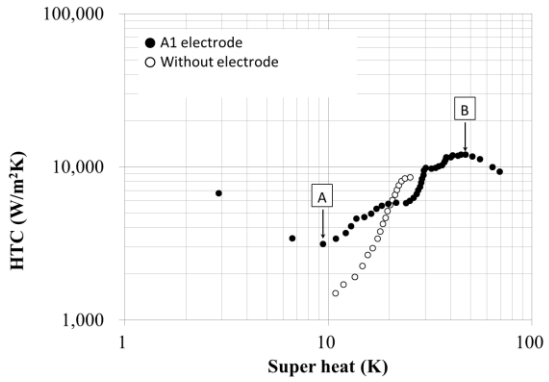

Fig. 6. Heat transfer coefficient (HTC) as a function of wall superheat at H = 400 μm and E= −5 kV/mm

(a)

(b)

Fig. 7. Bubble behavior (a) over the A1 electrode at H = 400 μm and E = −5 kV/mm (ΔT = 27.7 K, q = 19.5 W/cm^2), (b) over the smooth copper boiling surface (ΔT = 18.1 K, q = 9.7 W/cm^2)

The steady conditions were detected by the three temperatures in the copper block, which remained constant within the sensor uncertainty ± 0.04 K. The CHF was detected through the sudden increase in wall temperature, so that the three thermocouples never indicated steady conditions.

3. Experimental Results

3.1 Typical boiling curve with application of electric field

Figure 5 shows the heat flux as a function of wall superheat for an electrode height of 400 μm with the application of an electric field of −5 kV/mm. The corresponding heat transfer coefficient is shown in Fig. 6. The heat flux and heat transfer coefficient were compared with a pool boiling result without the electrode. As the superheat is increased, the first mode of heat transfer is EHD convection. At a certain value of superheat (Point A), vapor bubbles appear on the boiling surface. Above the superheat of 25 K, a sudden increase in the slope of the boiling curve is observed. At the maximum peak of the heat transfer coefficient (point B), the vapor begins to cover the whole boiling surface, and then the curve is reached a point of saturation resulting in CHF. The maximum heat flux is 65 W/cm^2 with the application of the electric field, and the maximum heat flux for pool boiling without the electrode is 22 W/cm^2. The theoretical maximum heat flux without the electrode provided by the hydrodynamic theory (Zuber, 1958) is

$$q_{\max} = \frac{\pi}{24} L\rho_v \left[\frac{\sigma g(\rho_l - \rho_v)}{\rho_v^{\,2}}\right]^{\frac{1}{4}} \left[\frac{\rho_l + \rho_v}{\rho_l}\right]^{\frac{1}{2}}. \qquad (6)$$

This equation gives $q_{\max}$ = 19.3 W/cm^2, with −14%.

Photographs of bubble behavior without the electrode and with the application of the

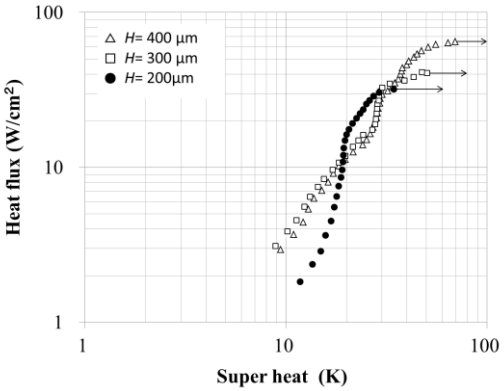

Fig. 8. Boiling curve for various electrode heights at E = −5kV/mm (case where A1 electrode is used)

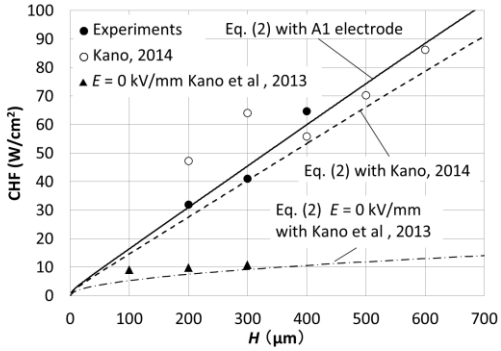

Fig. 9. Comparison of experimental results with Eq. (2) at E = −5kV/mm

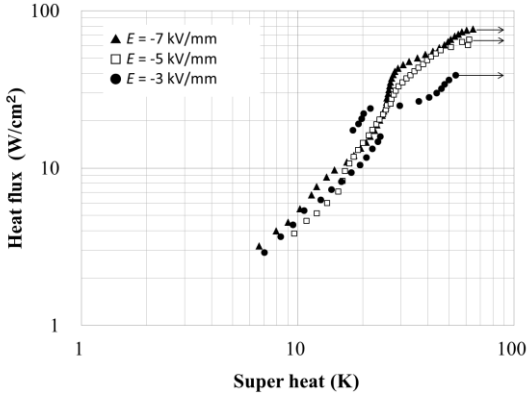

Fig. 10. Boiling curve for various electric field intensities at H = 400 μm (case where A2 electrode is used)

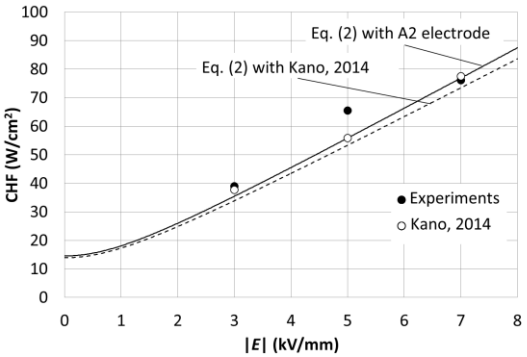

Fig. 11. Comparison of experimental results with Eq. (2) at H = 400 μm

electric field are shown in Fig. 7. Despite the superheat of 27.7 K, the bubble diameter with the application of the electric field is almost the same that at the superheat of 18.1 K. The author previously reported (Kano, 2014) more detailed bubble behavior in earlier electrode geometry (see Fig. 3). In addition, he found that the Kelvin–Helmholtz instability accelerated by the electrostatic pressure divided the vapor bubble into small bubbles and that the instability created a periodic thin liquid film on the boiling surface (which strongly increases the heat transfer). As noted above, mathematical expression was derived from these experimental results to predict maximum heat flux based on the addition of electrostatic pressure to the hydrodynamic theory, Eq. (2). For the present condition, calculation based on Eq. (2) provides $q_{\max, EHD}$ = 58 W/cm^2, which predicts an experimental maximum heat flux of 65 W/cm^2 with –12%.

3.2 Effects of electrode height, electric field, and total slit length on CHF

In Fig. 8, heat flux is plotted as a function of the wall superheat for different electrode heights at an electric field of –5 kV/mm. Heat transfer for EHD convection and the unstable behavior beyond the CHF are deleted from these figures and in the following boiling curves. Heat flux increases with the increase in the electrode height. The maximum heat flux is 65 W/cm^2 at an electrode height of 400 μm. The CHF as a function of electrode height is shown in Fig. 9. The CHF increases with the increase in the gap, H. The analytical result calculated by Eq. (2) almost agrees with the experimental results. In this figure, the experimental results measured by Kano (2014) are depicted. The results at 200 μm and 300 μm are higher than the analytical curve because the electric field deviates from the uniform distribution by the chamfered electrode edge (see Fig. 3). Despite the possibly nonuniform electric field distribution, the change in CHF over an electrode height of 400 μ m is estimated to be well under the given assumptions.

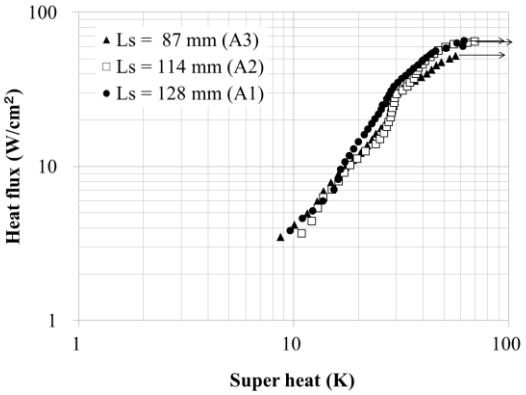

Fig. 12. Boiling curve for various total slit lengths at H = 400 μm and E = −5 kV/mm

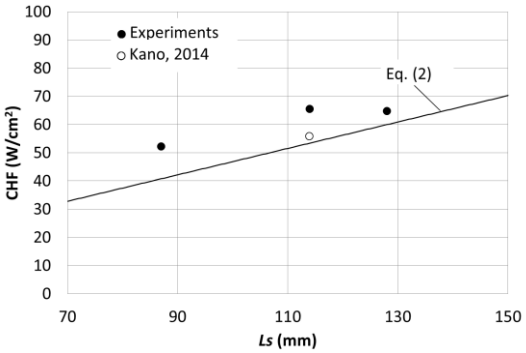

Fig. 13. Comparison of experimental results with Eq. (2) at H = 400 μm and E = −5 kV/mm

Misale et al. (2011) reported the effect on the CHF of confinement in a narrow horizontal space over the boiling surface. The upward boiling surface was confined by a face-to-face parallel unheated disc surface. The confinement sharply reduced the CHF. The CHF with the disc surface at the height of 500 μm was 5% of that without the electrode. Kano et al. (2013) also studied the confinement effect using the previously described electrode. The CHFs in the powered off condition at an electrode height of approximately 100–300 μm was shown in Fig. 9. In the experiment, HFE-7100 was selected as a working fluid. The CHFs are about 10 W/cm^2 which is 70% of the CHF without the electrode (14.7 W/cm^2). The analytical result calculated by Eq. (2) by referring to the physical properties of the liquid (EL-Genk and Bostanic, 2003) almost agrees with the experimental results. It is clear that even in the powered off condition, Eq. (2) predicts the experimental results well.

Fig. 10 shows the boiling curves as a function of electric field at an electrode height of 400 μm. The heat flux increases with the increase in the electric field. The maximum heat flux is 76 W/cm^2 at an electric field of –7 kV/mm. The CHF as a function of electric field is shown in Fig. 11. The results measured by Kano (2014) are also shown in this figure. The CHF increases with the electric field intensity E. The analytical result predicts the experimental results well.

Fig. 12 shows the boiling curves as a function of the total slit length at an electrode height of 400 μm and electric field of –5 kV/mm. The heat flux increases with the total slit length Ls. The maximum heat flux of 65 W/cm^2 is generated at both total slit lengths of 114 mm and 128 mm. The slit width Ws at the total slit length of 128 mm is 400 μm, which is narrower than that at the total slit length of 114 mm (Ws = 500 μm). This result indicates that the narrower slit width obstructed the bubble passage. The CHF as a function of the electric field is shown in Fig. 13. The results measured by Kano (2014) are also shown in this figure. The CHF increases with the total slit length Ls. The analytical result predicts the experimental results well.

4. Conclusion

In this study, the influence of a micro sized slit electrode design on the performance of boiling heat transfer was investigated experimentally, and the results were compared with previous analytical results. Managing the critical heat flux with electric field distribution was helpful for identifying key electrode designs that increase the range of regular functioning of the system.

The experimental results showed that the CHF increased with electrode height H, electric field E, and total slit length Ls. The maximum CHF with the application of the electric field was 76 W/cm^2 at a height of 400 μm, an electric field of –7 kV/mm, and a slit length 114 mm. This CHF was 3.5 times greater than the CHF for pool boiling without the electrode. The analytical results almost agreed with the experimental results, according to the variation in H, E and Ls (in the range 200 μm < H < 400 μm, –3 kV/mm < |E| < –7 kV/mm, 89 mm < Ls < 128 mm).

Acknowledgments

This study was partially supported by Grant-in-Aid for Scientific Research (C) from JSPS KAKENHI (No. 25420146) and by Industrial Technology Research Grant Program in 2006 from NEDO of Japan (No. 06B44014a).

The author would like to thank Mr. Kyohei Sato, Mr. Yohei Takahashi, and Mr. Tadashi chika (former graduate students at Yamagata University) for their assistance during the experiments.

The authors would like to thank Enago (www.enago.jp) for the English language review.

References

Allen, P. H. G., and Karayiannis, T. G., 1994, "Electrohydrodynamic Enhancement of Heat Transfer and Fluid Flow", Heat Recovery Systems & CHP, **15**(5), pp. 389-423.

Darabi, J., Ohadi, M. M., and DeVoe, D., 2001, "An electrohydrodynamic polarization micropump for electronic cooling", Journal of Microelectromechanical Systems, **10(1)**, pp. 98-106.

Darabi, J., and Ekula, K., 2003, "Development of a chip-integrated micro cooling device", Microelectronics Journal, **34(1)**, pp. 1067-1074.

EL-Genk, M. S., and Bostanici, H, 2003, "Saturation boiling of HFE-7100 from a copper surface, simulating a microelectric chip", International Journal of Heat and Mass Transfer, **46**, pp. 1841-1854.

Hristov, Y., Zhao, D., Kenning, D. B. R., Sefiane K., and Karayiannis T. G., 2009, "A study of nucleate boiling and critical heat flux with EHD enhancement", Heat Mass Transfer, **45**, pp. 999-1017.

Jones, T. B., 1978, "Electrohydrodynamically Enhanced Heat Transfer in Liquids－A review", Advances in Heat Transfer, **14**, pp.107-148.

Kano, I., and Takahashi, Y., 2013, "Effect of electric field generated by micro sized electrode on pool boiling", IEEE Transactions on Industry Applications, **49**(6), pp. 2382-2387.

Kano, I., Higuchi, Y., and Chika, T., 2013, "Development of boiling type cooling system using electrostatics effect", Trans. ASME Journal of Heat Transfer, **135**, pp. 091301(1-8).

Kano, I., 2014, "Effect of electric field distribution generated in a micro space on pool boiling heat transfer", Trans. ASME Journal of Heat Transfer, in print.

Laohalertdecha, S., Naphon, P., and Wongwises, S., 2007, "A Review of Electrohydrodynamic Enhancement of Heat Transfer", Renewable & Sustainable Energy Reviews, **11**, pp. 858-876.

Marco, D. I., P., and Grassi, W., 1993, "Saturated Pool Boiling Enhancement by Means of an Electric filed", Enhanced Heat Transfer, **1**(1), pp. 99-114.

Misale, M., Guglielmini, G., and Pariarone, A., 2011, "Nucleate boiling and critical heat flux of HFE-7100 in Horizontal narrow spaces", **35**, pp. 772-779.

Moghaddam, S., and Ohadi, M. M., 2005, "Effect of electrode geometry on performance of an EHD thin-film evaporator", Journal of Microelectromechanical Systems, **14(5)**, pp. 978-986.

Panofsky, W. K. H., 1962, "Classical Electricity and Magnetism", Second Edition, Dover Publications, pp. 111-116.

Pickard, W. F., 1963, "Ion-drag pumping. I. Theory", Journal of Applied Physics, **34(**2), pp. 246-250.

Pickard, W. F., 1963, "Ion-drag pumping. II. Experiment", Journal of Applied Physics, **34(**2), pp. 251-258.

Saville, D. A., 1997, "Electrohydrodynamics: The Taylor-Melcher Leaky Dielectric Model", Annual. Review on Fluid Mechanics", **29**, pp. 27-64.

Stuetzer, O. M., 1959, "Ion drag pressure generation", Journal of Applied Physics, **30**(7), pp. 984-994.

Tong, L. S., and Tang, Y. S., 1997, Boiling Heart Transfer and Two-Phase Flow, Second Edition, Taylor & Francis, pp. 37-40.

Zuber, N., 1958, "On the stability of boiling heat transfer", Trans ASME Journal of Heat Transfer, **80**, pp. 711-720.